A Novel Control Scheme for Induction Generator Based Stand-alone Micro Hydro Power Plants

Hanumanthu Kesari and Natarajan Kumaresan*

Department of Electrical and Electronics Engineering, National Institute of Technology, Tiruchirappalli, India 620015
E-mail: kesarihanu.05@gmail.com; nkumar@nitt.edu
**Corresponding Author*

Received 25 December 2022; Accepted 04 July 2023;
Publication 26 August 2023

Abstract

A system comprising of a hydraulic turbine (HT) driven induction generator with excitation capacitor (IGEC) has been proposed for providing electricity to the residents living in remote areas and steep terrains, wherein the grid connection is unviable. The available water resource in such locations is effectively utilized and the load on the generator terminals is set, based on the requirement of the consumer demand. A method has been formulated for the estimation of excitation capacitor and rotor speed for ensuring nominal voltage and frequency at the generator terminals, regardless of variation in the consumer load. This design procedure is based on the analysis of IGEC employing the binary search algorithm (BSA). The logical way of arriving at the range of per unit (*pu*) speed to start the BSA has also been illustrated. A closed-loop control scheme has also been formulated, by taking generator voltage as the feedback variable and comparing the voltage set limits V_{min} and V_{max}. Accordingly, a controller action is initiated to add or disconnect the flexible loads. An available mathematical modeling of HT has been modified

Distributed Generation & Alternative Energy Journal, Vol. 38_6, 1791–1814.
doi: 10.13052/dgaej2156-3306.3864

suitably and by using this model, the functioning of the proposed system with respect to the HT characteristics and generated frequency of IGEC has also been investigated. Using a MATLAB/Simulink software, the successful functioning of the proposed system has been demonstrated with typical operating conditions. The predetermined values and simulated observations are amply supported with the laboratory results conducted on a 3-phase, 3.7 kW IGEC.

Keywords: Induction generators, energy conversion, hydroelectric power generation, power conversion, distributed generation.

1 Introduction

In the last two to three decades, planning, designing and installing of various forms of renewable energy sources are being increasingly emphasized world over, to bring in a totally pollution free environment, for healthy and comfortable living. The international energy agency anticipates that the capacity of the renewable electricity to grow by over 60%, and account for almost 95% of the global power capacity by 2026 [1]. This is equivalent to the current combined global capacity of fossil fuels and nuclear power. In this context, deployment of Electric vehicles is fast picking up and replacing, diesel and petrol driven ones. Among the renewables, solar photovoltaic systems dominate, followed by wind, hydropower and bioenergy.

The hydroelectric power systems range from massive ones of hundreds of MW rating to power an entire state, to small ones of tens of kW which would fulfill the domestic as well as agricultural needs of a local community, particularly those in remote villages and hilly areas, far away from main power lines. However, it is to be mentioned that the installation of large hydro plants causes a vast deforestation and destruction of animals and green lands. The present emphasis being to preserve natural resources, deployment of micro hydro power plants (MHPP) as a distributed generation, which does not require a reservoir or large civil construction work, is gaining popularity. So, MHPP is also being promoted along with wind energy conversion systems and solar photovoltaic systems to enhance the installation of renewable power plants.

The first important step in installing MHPP, involves a logical way of fixing a suitable hydraulic turbine (HT) to drive the generator. In this regard, Jawahar et al. have made an exhaustive review of turbines available in India and abroad, used for small and MHPP, along with the details of the

manufacturers [2]. Elbatran et al. have studied the economic analysis and selection of appropriate turbines suitable for this application along with its operation and performance [3]. Many researchers have developed mathematical modeling of the HT for predicting its performance [4–7] and one such model is considered in this paper. Shalvi Tyagi et al. have also proposed a permanent magnet synchronous generator (PMSG) based system for standalone small hydro plants [8]. References [9, 10] present a comprehensive review of the operation and control of MHPP. It is to be noted that the size and cost of PMSG is higher compared to the induction generator for ratings less than 100 kW [11]. Induction machines are also more robust and available on-shelf. Hence, several authors have dealt with induction generator with excitation capacitor (IGEC) to be operated in self-excited mode for HT driven electricity generation [12].

The mechanical output power from HT is constant for a fixed head and discharge. So, with a view to ensure a reliable and efficient method of operating the MHPP employing IGECs, various power converter topologies have been proposed, namely, (i) 3-phase AC chopper connected between generator and dump load [13–15], (ii) diode bridge rectifier with chopper [16], (iii) DSTATCOM at generator terminals [17–19], (iv) DSTATCOM with hybrid topology [20], (v) STATCOM with battery energy storage system [21] and (v) battery-supported unified power quality controller [22]. Further, the excess energy available more than the consumer load has been utilized for space heating, battery charging and water pumping etc, instead of wasting it in dump load [13, 15, 19, 21, 22]. In all the available literature, the MHPP is always operated at full load conditions. However, it is observed that the requirement of the consumer load is not always close to the full load condition and it varies widely from nearly light load to the rated capacity. Hence, an attempt is made in this paper for the comprehensive operation and control of HT driven IGEC based on the requirement of the consumer load with different water flow rates.

In this paper, a method is devised for selection of excitation capacitor and speed at which the induction generator has to be driven in order to maintain the power at the generator terminals constant by maintaining the stator voltage and frequency at their rated values. However, a study of the characteristics of the HT [5–7], shows that the generator should be operated with different speeds to extract maximum possible power, for a given water discharge. Hence, two cases are considered for the IGEC driven by uncontrolled HT, feeding power to rural and remote places. The first one is the constant power operation in which the load voltage and frequency

are retained at their nominal values. The second one is the MPPT wherein only the stator voltage is maintained at its nominal value and it can be used for frequency insensitive loads such as space heating, lighting, low voltage DC appliances, which demand only regulated voltage. The functioning of the overall system has been exemplified with exhaustive simulation and validated through experimental results. Thus, the implementation of the configuration and control of HT driven induction generator system would substantially support the advancement towards the UN's sustainable development goal of achieving affordable clean energy (SDG-7) by 2030.

The remainder of this paper is structured as follows: Section 2 describes the proposed system along with its control strategy. The prediction of IGEC's steady state performance deploying its equivalent circuit, followed by a design procedure for estimation of speed, excitation capacitor and mathematical modeling of prime mover is described in Section 3. The effectiveness of the proposed system has been verified through simulation and authenticated with augmented experimental results in Section 4. Section 5 outlines the salient points and findings of the proposed method.

2 Proposed System Description and Control Strategy

The overall schematic of the proposed system is shown in Figure 1. It consists of a hydraulic turbine used as a prime mover to drive a 3-phase delta connected IGEC for supplying consumer loads along with other flexible loads (FLs). The mechanical power output of HT being constant for a given water head (*H)* and water flow rate (*Q*), the power output at the generator terminals needs to be maintained constant for any change in the consumer load. Otherwise, the generator would accelerate, resulting in rise in voltage and frequency. On the other hand, generator operation would cease if consumer load is higher. So, in this system FLs are considered, to assist in retaining the set power at the generator terminals, which in turn requires the nominal value of voltage and frequency to be maintained.

In order to optimally utilize the available water resource like lakes, it is also proposed to operate the system with different outputs, based on the consumer demand by appropriately controlling the water flow rates. Firstly, the speed and capacitor values are to be estimated to get the rated voltage and frequency at the generator terminals for different load settings. Such an estimation procedure has been developed in this work utilizing the steady-state equivalent circuit of the generator [23] and binary search algorithm (BSA) [24–28]. These estimated values are stored as a look-up table in the

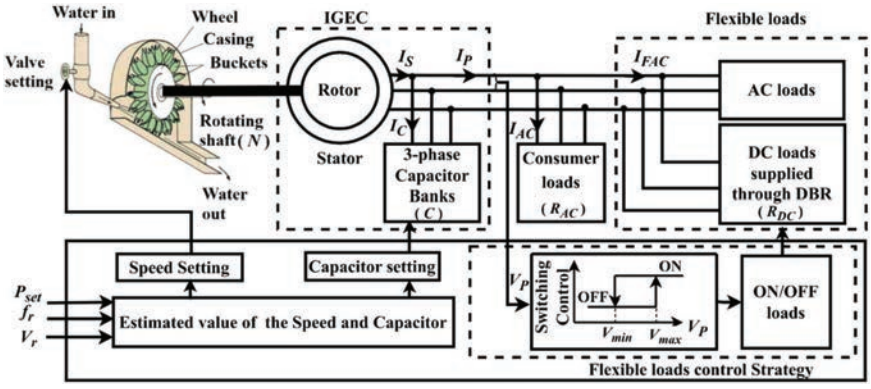

Figure 1 Proposed induction generator based MHPP system. P_{set}: Set power; f_r: Rated frequency; V_r: Rated voltage.

controller shown in Figure 1. Then, based on the requirement of consumer demand, the controller can set the appropriate value of speed by controlling the water flow and the value of excitation capacitance, by switching in/out the capacitor banks. Subsequently, for the given output, the stator line voltage V_P is taken as the feedback variable for controlling the FLs. To prevent the oscillations, a hysteresis band is given for the voltage limit and hence the IGEC gives nominal output voltage. It is to be noticed that the frequency of IGEC predominantly depends on speed [24, 29] and hence frequency is maintained at its nominal value by running the generator at fixed speed. The successful functioning of the entire system has been substantiated with HT modeling through simulation and validated with experimentation by emulating the HT with DC motor.

3 Analysis and Design of the Proposed System

The equivalent circuit of IGEC shown in Figure 2 has been considered along with the parameters of a three phase, 3.7 kW, 230 V, delta connected IGEC given in Table 1 for the performance evaluation and experimental investigations. All reactances are corresponding to the rated frequency in the equivalent circuit and X_m is the per phase magnetizing reactance in Ω. Further, $a = (f_g/f_r)$ is per unit (*pu*) frequency, and $b = N/N_S$ is *pu* speed. f_g and f_r are generated and rated frequencies, respectively, in Hz, N and N_S are the actual rotor speed and synchronous speed corresponding to rated frequency, respectively, in rpm. The magnetization characteristics of IGEC

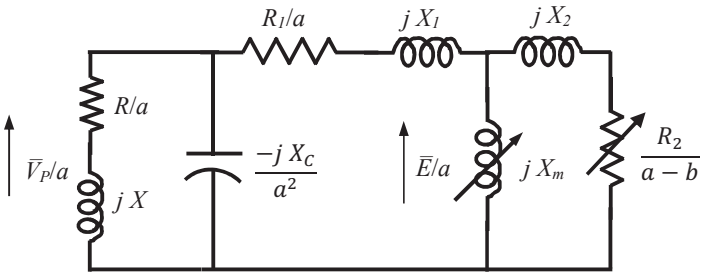

Figure 2 Equivalent circuit of IGEC.

Table 1 Per phase equivalent circuit parameters of IGEC

Per Phase Parameter	Value
Stator Resistance (R_1)	1.30 Ω
Rotor Resistance (R_2)	1.75 Ω
Stator leakage reactance (X_1)	2.60 Ω
Rotor leakage reactance (X_2)	2.60 Ω
Critical magnetizing Reactance (X_{mc})	75 Ω
Rated frequency (f_r)	50 Hz

obtained experimentally is

$$\frac{\overline{E}}{a} = -296.8 \times 10^{-10} X_m^6 + 761 \times 10^{-8} X_m^5 - 785.7 \times 10^{-6} X_m^4 + 40.79 \times 10^{-3} X_m^3 - 111.1 \times 10^{-2} X_m^2 + 12.95\, X_m + 245.9 \quad (1)$$

3.1 Estimation of N and C

A method has been developed for the estimation of *N* and *C*, so that the IGEC operates with rated voltage and frequency for a specified power. Firstly, the load resistance, *R* and reactance, *X* have to be computed for the given power, P_{set} by using the generator voltage as the reference phasor. Then, under steady state condition, the admittance of the circuit shown in Figure 2 can be considered as [24],

$$\frac{1}{\overline{Z}_{SR}} + \frac{1}{jX_m} = 0 \quad (2)$$

$$\frac{1}{\overline{Z}_{SR}} = \frac{1}{\overline{Z}_S + \overline{Z}_{LC}} + \frac{1}{\overline{Z}_R} \quad (3)$$

where

$$\overline{Z}_S = \left(\frac{R_1}{a}\right) + jX_1, \quad \overline{Z}_R = \left(\frac{R_2}{a-b}\right) + jX_2, \quad \overline{Z}_L = \left(\frac{R}{a}\right) + jX,$$

$$\overline{Z}_C = \left(\frac{-jX_C}{a^2}\right), \quad X_C = \frac{1}{2\pi f_r\, C} \quad \text{and} \quad \overline{Z}_{LC} = \frac{\overline{Z}_L \overline{Z}_C}{\overline{Z}_L + \overline{Z}_C}$$

The real and imaginary parts of admittance given in (2) are

$$real\left(\frac{1}{\overline{Z}_{SR}}\right) = 0 \tag{4}$$

$$img\left(\frac{1}{\overline{Z}_{SR}}\right) = \frac{1}{X_m} \tag{5}$$

Equation (4) can be utilized for evaluating the unknown value of *b* for the given value of *a* and other specified parameters of the machine, capacitor value and load, by adopting the BSA described in [24]. The salient steps of BSA for the determination of *b* and X_m are also given in the flowchart of Figure 3. To start this algorithm, the initial values of b_{min} and b_{max} are needed. Here, b_{min} is estimated by ignoring R_1, X_1 and X_2 in Figure 2.

The resultant expression for b_{min} is arrived at as

$$b_{min} = a + R_2\ real\left(\frac{1}{\overline{Z}_{LC}}\right) \tag{6}$$

Considering the maximum operating slip of 6% for IGEC, the value of b_{max} is taken as 1.06 times of b_{min}. Subsequently X_m can be calculated using (5) and induced emf can be evaluated using (1) of IGEC. Then, the stator voltage per phase can be evaluated using

$$\overline{V}_P = \overline{E}\frac{\overline{Z}_{LC}}{\overline{Z}_S + \overline{Z}_{LC}} \tag{7}$$

During this process, the voltage magnitude computed from (7) is checked with the rated value for each excitation capacitor value for the given power. The process is stopped, if the voltage calculated is found within the tolerance. Else, the evaluation process will be repeated for other values of excitation capacitors. This process of estimation of *N* and *C* is depicted in Figure 3. The outputs, namely, speed and excitation capacitor values thus obtained from this estimation can be formed as a look-up table for the control of

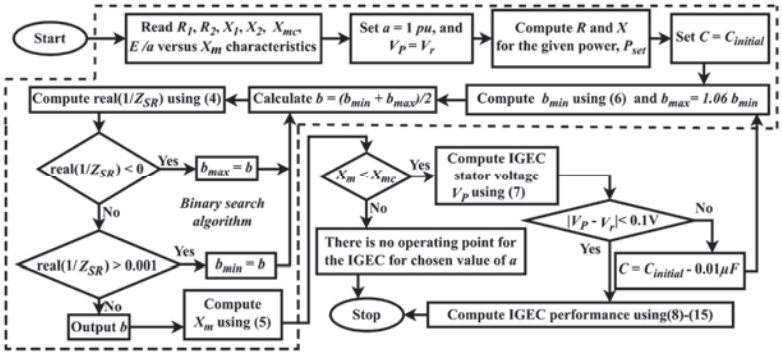

Figure 3 Estimation of b and X_m and the performance of IGEC using BSA.

the proposed system shown in Figure 1. Further, the performance quantities of IGEC can be determined using the following equations derived from the circuit of Figure 2.

$$\text{Load current, } \overline{I}_P = \frac{\overline{V}_P/a}{\overline{Z}_L} \tag{8}$$

$$\text{Capacitor current, } \overline{I}_C = \frac{\overline{V}_P/a}{\overline{Z}_C} \tag{9}$$

$$\text{Stator current, } \overline{I}_S = \overline{I}_P + \overline{I}_C \tag{10}$$

$$\text{Rotor current, } \overline{I}_R = \frac{\overline{E}/a}{\overline{Z}_R} \tag{11}$$

$$\text{Generated power output, } P_e = 3\ real(\overline{V}_P\ \overline{I}_P^*) \tag{12}$$

$$\text{Stator copper loss, } P_S = 3\ |\overline{I}_S^2|\ R_1 \tag{13}$$

$$\text{Rotor copper loss, } P_R = 3\ |\overline{I}_R^2|\ R_2 \tag{14}$$

$$\text{Mechanical power input, } P_M = 3\ |\overline{I}_R^2|\ R_2\ \left(\frac{b}{a-b}\right) \tag{15}$$

Also $P_M = P_e + P_S + P_R$.

3.2 Modeling of Hydraulic Turbine

To make a realistic study on the working of the proposed system shown in Figure 1, the mathematical modeling of the HT has been considered [7]

which is intended to drive the IGEC. The literature shows that the operating characteristics of the propeller-type or semi-Kaplan turbine with fixed blades and fixed guide vanes HT used in MHPP [4] resembles wind turbine characteristics with zero pitch angle [23]. In this regard, the available hydraulic power of HT is ρQgH which can also be expressed as

$$P_h = 0.5\rho A V_w^3. \tag{16}$$

where ρ represents the specific density of water (1000 kg/m^3 at 39.2°F or 4°C), *A* being the area swept (πR_{HT}^2) by the rotor blades in m^2, R_{HT} denotes the radius of the blades in m, V_{w} is the water flow speed or velocity of water flow in m/s which can be expressed as $V_w = \sqrt{2gH}$ and also $V_w = Q/A$, *Q* is the discharge or water flow rate in m^3/s, g represents acceleration due to gravity (9.806 m/s^2), *H* represents the net water head in m.

The mechanical power output from the turbine, P_m equal to $\eta(\lambda, Q)P_h$, which can be expressed as

$$P_m = 0.5\ \eta(\lambda, Q)\rho A V_w^3. \tag{17}$$

where η represents hydraulic turbine efficiency which depends on λ and water flow rate, *Q*.

The expression for steady-state efficiency of the semi-Kaplan turbine obtained experimentally is given as [7]

$$\eta(\lambda, Q) = \frac{1}{2}\left[\left(\left(\frac{90}{\lambda_i}\right) + Q + 0.78\right) e^{-50/\lambda_i}\right](3.33\ Q) \tag{18}$$

where $\frac{1}{\lambda_i} = [\frac{1}{\lambda+0.089} - 0.035]$ and $\lambda = R_{HT}\ A\omega/Q$ or $\lambda = R_{HT}\omega/V_w$ where ω is the rotor speed in rad/s.

Then the mechanical torque produced by the HT is

$$T_m = P_m/\omega. \tag{19}$$

In order to get the optimal rotational speed of the turbine for the given discharge *Q*, (17) has to be differentiated with respect to ω and equating it to zero. At this speed, the turbine operates at maximum efficiency and hence the maximum mechanical power output can be drawn. The step-by-step procedure thus formulated for obtaining the mechanical power output versus rotational speed of the HT for the given water flow rate is shown in Figure 4.

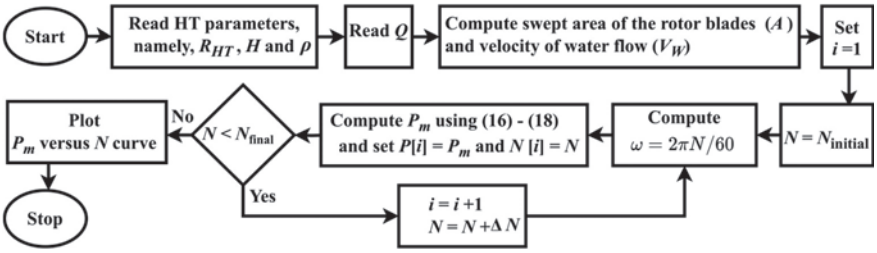

Figure 4 Procedure for evaluating the mechanical power output versus rotor speed characteristics of the HT. $\Delta N = 10$ rpm, $N_{final} = 2100$ rpm.

Table 2 Estimation of speed, excitation capacitance and performance parameters to maintain the stator voltage of 230V at 50 Hz for different load settings

R, Ω	N, rpm	pre/sim/exp	$C, \mu F$	V_P, V	f_g, Hz	P_e, kW	I_S, A	I_P, A	I_C, A
165	1519	pre	63.04	230.0	50.0	0.962	8.2	2.4	7.9
		sim	63.04	239.4	50.0	1.037	8.3	2.5	7.8
		exp	65.37	224.2	50.2	0.918	8.4	2.3	8.0
82.5	1536	pre	66.70	230.0	50.0	1.923	9.6	4.8	8.3
		sim	66.70	231.8	50.0	1.956	9.3	5.0	7.7
		exp	69.86	223.9	50.4	1.823	9.7	4.5	8.5
55.0	1554	pre	71.75	230.0	50.0	2.885	11.5	7.2	8.9
		sim	71.75	230.6	50.0	2.904	10.9	7.4	8.1
		exp	73.08	223.8	50.6	2.731	11.5	6.7	9.3
41.25	1572	pre	78.21	230.0	50.0	3.847	13.7	9.6	9.7
		sim	78.21	230.8	50.0	3.878	13.8	9.7	9.1
		exp	80.66	226.8	50.7	3.743	14.0	9.1	10.5

Note: pre: results obtained through the evaluation method given in Figure 3; sim: simulation results; exp: experimental results.

4 Results and Discussions

Firstly, N and C are estimated using the proposed method described in Figure 3 for the test machine. The results thus obtained for typical load resistances are given in Table 2. Subsequently these values are verified using simulation and experiment conducted in the laboratory to show the effectiveness of the proposed method of analysis and its successful functioning.

4.1 Simulation Set-up

For the simulation study, the parameters of the machine given in Section 3 along with the saturation curve obtained experimentally for the test machine

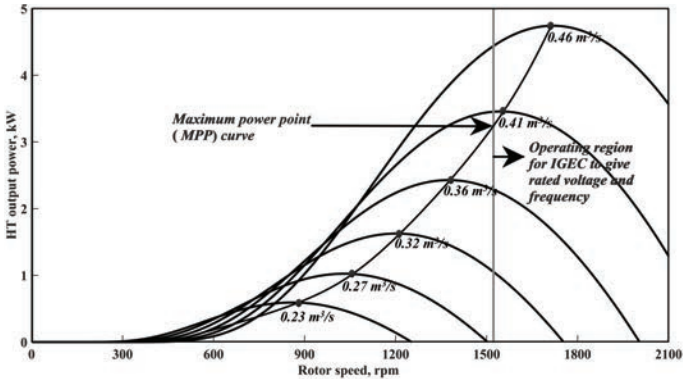

Figure 5 Characteristics of hydraulic turbine.

has been used suitably in the Induction machine model available in MATLAB/SIMULINK. Then, the excitation capacitors are connected at the stator terminals for the excitation of the generator. A three-phase delta connected resistive loads connected at the stator terminals are used as consumer load. Then the performance of IGEC for various operating conditions given in Table 2 has been verified using simulation set-up and the corresponding simulated results are also given in this Table.

To assess the functionality of the proposed system shown in Figure 1. The HT parameters chosen to drive the 3.7 kW IGEC considered in this paper are: $H = 1$ m, $R_{HT} = 0.27$ m, base $V_W = 2$ m/s, base rotational speed $= 1750$ rpm, mechanical power output $(P_m) = 5$ kW, maximum power at base water flow velocity is 0.95 *pu*, moment of inertia, $J = 0.0004$ kg-m^2. Then using the process described in Figure 4 and typical parameters, a plot of mechanical power output versus rotor speed for different water flow rates thus obtained for HT is shown in Figure 5. It can be noticed from this figure that, there exist a point on the characteristics where the mechanical power output is maximum (MPP) for each water flow rate. A wind turbine model available in the MATLAB has been appropriately modified to accommodate the HT characteristics described in (17)–(19) with the chosen parameters. The output of HT model gives mechanical torque for given water flow rate (Q) and the negative value of this torque is given as an input to the Induction machine model for operating as IGEC.

The FLs, which are controllable [30–32], are also connected at the stator terminals apart from the consumer load. For MATLAB/SIMULINK model verification, the FLs have been simulated by connecting 15 numbers ($\mathrm{FL}_{\max}$)

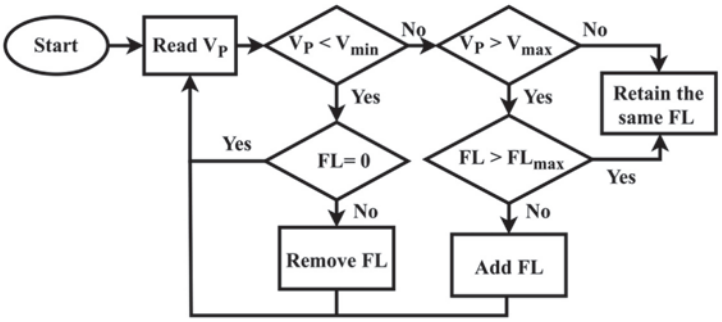

Figure 6 Flexible load (FL) control strategy for the proposed system shown in Figure 1. $\mathrm{FL_{max}} = 15$.

of resistive loads each of 200 W supplied through the diode bridge rectifier. The per phase resistive load settings of 165 Ω, 82.5 Ω and 55 Ω are used to simulate the step-change in the consumer loads (R_{AC}). The control strategy for switching in/out these FLs for any alterations in the consumer load is shown in Figure 6. This control strategy has been implemented in simulation by employing embedded MATLAB function to maintain the stator line voltage within the upper (V_{max}) and lower (V_{min}) bands. The hysteresis band for stator voltage is chosen as $\pm 3\%$ of its nominal value to avoid chattering.

The simulation has been carried out for various operating conditions and the working of the system is observed. For the sake of brevity, results obtained for a total load of about 2.885 kW and 1.923 kW at the generator terminals are shown in Figure 7. Figure 7(a) shows the dynamic response of the system with the water flow rate of $Q = 0.41$ m^3/s so that HT drives the IGEC for supplying a total load at the generator terminals, P_e equal to 2.885 kW. It can be noted from this figure that in the Interval-I the consumer load is 0.953 kW with $R_{AC} = 165$ Ω. A balance power of 1.981 kW is supplied to FLs. In the Interval-II at t = 2 s the consumer load is increased from 0.953 kW to 1.943 kW by step changing of R_{AC} from 165 Ω to 82.5 Ω. Then the controller monitors the stator voltage and disconnects the FLs so that the generated power is maintained corresponding to the value for the given water flow rate. Similar observation has been noted in the Interval-III when the consumer load is further increased to 2.885 kW at t = 4 s by step changing of R_{AC} from 82.5 Ω to 55 Ω. For clarity, Figure 7(a) also includes a zoomed version of the stator voltage and current as well as the DC voltage and current.

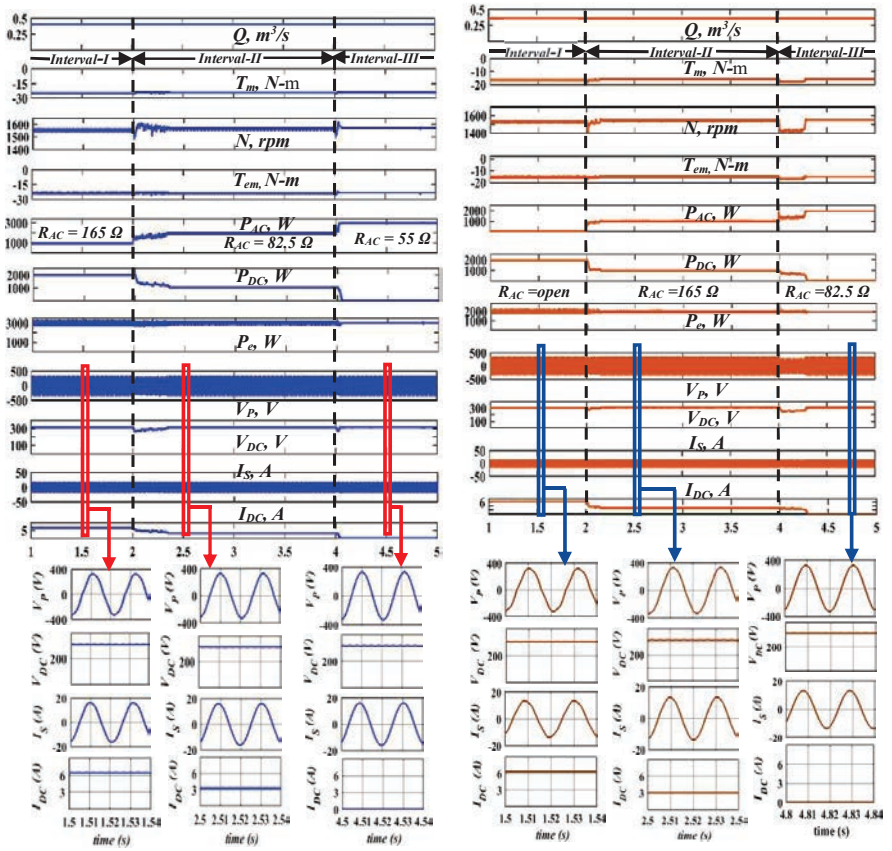

(a) (b)

Figure 7 Dynamic response of the system for step change in the consumer load. (a) $Q = 0.41$ m^3/s. (b) $Q = 0.37$ m^3/s. T_{em}: electromagnetic torque of IGEC, P_{AC}: consumer load power, P_{DC}: DC load power, V_{DC}: DC load voltage and I_{DC}: DC load current.

To further show the effectiveness of the functioning of the proposed system, simulation has also been carried out for water flow rate of $Q = 0.37$ m^3/s so that HT drives the IGEC for supplying a total load at the generator terminals, P_e of about 1.923 kW. Simulated results starting from no consumer load to a load of 1.923 kW with $R_{AC} = 82.5\ \Omega$ are also given in Figure 7(b). Figure 7 clearly shows that the total generated power at any given instant is maintained close to the set value by adding or removing the FLs for the given water flowrate of HT. Thus, the IGEC delivers the nominal voltage

(230 ± 3% V) and frequency (50 ± 2% Hz) by the closed loop control. Further the DC voltage variation is ±3% as the generator terminal voltage is maintained with the nominal value. But the DC current varies based on the value of consumer loads. The Simulation has also been performed for step decrease in consumer loads and successful functioning of the proposed system has been noted.

4.2 Experimental Investigations

For the system depicted in Figure 1, an experimental setup has been created in the lab that uses a separately excited DC motor as the primary mover to drive the IGEC. Then the IGEC was made to operate at a specific speed with the capacitor close to the estimated value based on the availability in the laboratory. Table 2 also gives these experimental results, which also agree closely with the calculated values and simulation results thereby validating the proposed method of analysis and design described in Section 3.

By looking into the characteristics of HT shown in Figure 5 for reduced power of, say $Q = 0.36$ m^3/s, the peak power occurs at 1400 rpm. For this speed, the generated frequency of IGEC is less than 50 Hz which can be inferred by the following expression [24, 29]

$$f_g = (PN/120) + (a - b)f_r \tag{20}$$

where *P* is the number of poles of IGEC.

Hence at light load conditions, it is not possible to operate IGEC to give rated frequency at or near MPP of HT. So, for frequency insensitive loads, the proposed system can be operated close to MPP with rated voltage alone. These aspects are given in Table 3 for a typical load of 2.0 kW along with

Table 3 Performance of HT driven IGEC at 2 kW, $V_P = 230$ V

Operating Condition	pre/ sim/ exp	R (Ω)	Q (m^3/s)	N (rpm)	C (μF)	V_P (V)	f_g (Hz)	P_e (kW)	I_S (A)	I_P (A)	I_C (A)
	pre	82.5	0.36	1400	95.30	230.1	45.5	1.925	11.8	4.8	10.8
X	sim	82.5	–	1407	95.30	227.1	45.6	1.882	11.9	4.5	10.6
	exp	82.5	–	1400	98.00	228.1	45.8	1.892	12.5	4.6	11.6
	pre	82.5	0.37	1536	66.70	230.0	50.0	1.923	9.6	4.8	8.3
Y	sim	82.5	–	1549	66.70	232.7	50.3	1.970	9.5	4.7	8.2
	exp	82.5	–	1536	69.86	223.9	50.4	1.824	9.7	4.5	8.6

Note: *X*: operation at MPP, *Y*: operation of IGEC to deliver the nominal voltage and frequency

the predetermined and simulated values. It can be inferred from the table that the water discharge (Q) should be on the higher side for simultaneously satisfying both voltage magnitude and frequency. Further, the value of C is more at MPP and there is a possibility of IGEC coming out of excitation since the operating speed is lower than its rated value.

To show the efficacy of the proposed system under step change in consumer load, experiments were also conducted in the laboratory for the typical operating conditions of simulated results given in Figure 7. Here, the IGEC was made to run at constant speed using a separately excited DC motor. For experimental verification, a 3-phase resistive load box available in the laboratory with load setting of 165 Ω, 82.5 Ω, 55 Ω was connected at the stator terminals. The FLs have been simulated by connecting two resistive loads of 48 Ω and 90 Ω available in the laboratory fed through diode bridge rectifier module (MD8TU6012). The purpose of this arrangement is to demonstrate the operation of the proposed system to maintain the nominal voltage i.e., 230 V and 50 Hz at the generator terminals with different combination of consumer and FLs, for the specified value of load, speed and excitation capacitance.

Experimentally obtained performance quantities namely stator line voltage (V_P), DC load voltage (V_{DC}), generated frequency (f_g), stator line current (I_S), load current (I_P), consumer load current (I_{AC}), DC load current (I_{DC}), generated power (P_e), DC load power (P_{DC}), rotor speed (N), consumer load resistance (R_{AC}), DC load resistance (R_{DC}) along with the simulated ones for variation in the consumer load power (P_{AC}) for a total load of 2.885 kW are shown in Figure 8. Figure 8(a) show that V_P, f_g and V_{DC} are maintained at their nominal values with allowable tolerance for variations in the consumer load. Figures 8(b) and 8(c) reveal that the I_S and I_P are almost constant whereas I_{DC} and P_{DC} decreases, and I_{AC} increases with increase in consumer load, P_{AC}. It is also noted that the generated power which is the sum of consumer load power and DC load power is maintained at its set value for the given operating condition. Thus, a close agreement between the experimental results with simulated/predetermined ones validate the proposed method of operating IGEC for MHPP and their design and analysis.

Experiments have also been conducted for step change in the consumer load and appropriately altering the FLs for given power settings. The captured voltage and current waveforms at the IGEC terminals and on the DC load side for two power settings are given in Figure 9. Figure 9(a) corresponds to a total power setting of 2.885 kW and for a consumer load R_{AC} changing from

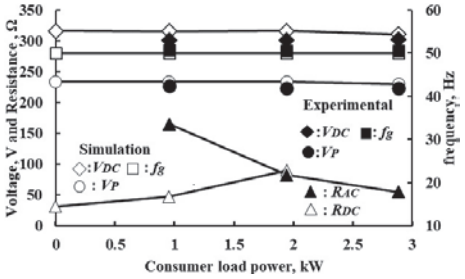

(a) V_{DC}, f_g, V_P, R_{AC} and R_{DC} with consumer load power.

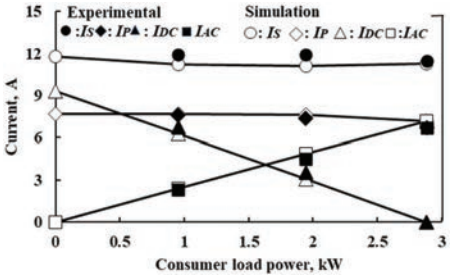

(b) I_S, I_P, I_{DC}, and I_{AC} with consumer load power.

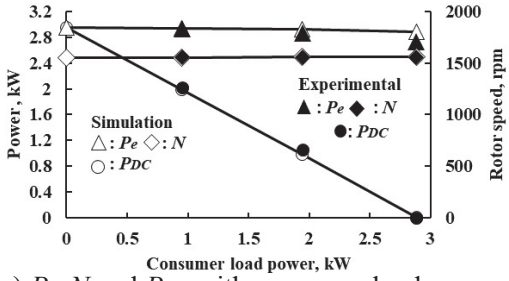

(c) P_e, N and P_{DC} with consumer load power.

Figure 8 Steady state performance characteristics of the system for change in consumer load.

165 Ω to 82.5 Ω. Similarly, Figure 9(b) corresponds to a total power setting of 1.923 kW and for a step change in consumer load R_{AC} from no-load to 165 Ω. It can be noticed from this figure that the stator line voltage and DC load voltage are held at their nominal values even when the consumer load varies. The DC load power and hence DC load current is decreased with the increase in consumer load thereby maintaining the generated power as well as the stator current constant at IGEC terminals. Figure 10 shows the photograph of experimental setup of the proposed system.

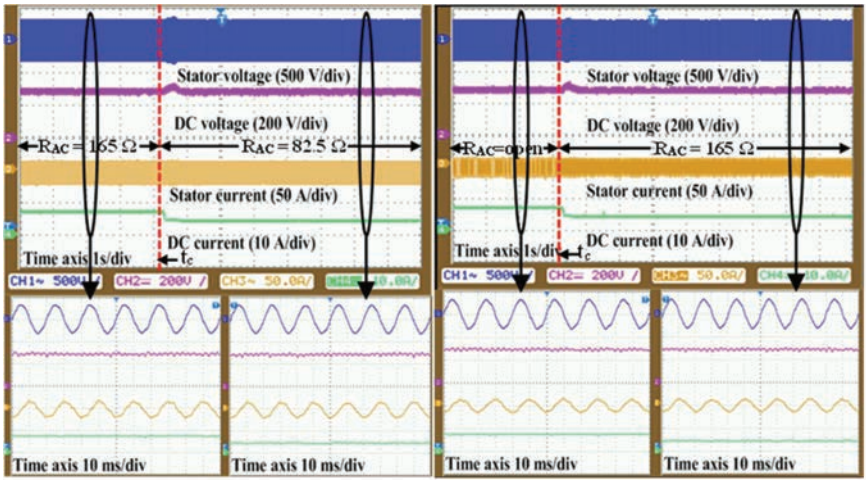

(a) (b)

Figure 9 Experimental waveforms of the proposed system for step change in the consumer load. (a) power setting of 2.885 kW. (b) power setting of 1.923 kW. t_c: Instant at which the consumer load change is initiated.

Figure 10 Experimental setup of the proposed system. 1-DC motor, 2-Induction Generator, 3-three phase auto transformer, 4-Fluke 345 clamp meter, 5-Capacitor bank, 6-consumer load, 7-Digital storage oscilloscope, 8-three phase diode bridge rectifier, 9-multi meter, 10-High voltage differential probe, 11-Hall effect current probe, 12-DC loads.

5 Conclusion

The people living in remote sites and steep terrains have limited access to electricity since connecting them to the grid is both not easy and economical. The installation of MHPPs is one of the best alternatives and sustainable solution to provide power to such small communities as the operation of MHPPs can be carried out in small streams, rivers, or channels without causing any environmental effect. In view of these aspects, this paper has proposed the generation of electricity using a HT driven induction generator system to meet the basic needs such as lighting, cooking and water heating etc. Further, it envisaged to operate this proposed system with variable load on the generator based on the consumer load requirement for the efficient utilization of the available water resources. Thus, the main requirement of the system is to maintain the nominal voltage and frequency at the generator terminals for any variation of the consumer loads. Hence, a methodology has been designed for the estimation of rotor speed and the value of excitation capacitor for the given power output of IGEC to satisfy such requirements. The design process is initiated by taking the value of *pu* frequency, *a* equal to 1 (corresponding to the rated frequency of 50 Hz). Then the unknown parameters namely *pu* speed, *b* and magnetizing reactance X_m are evaluated using BSA. A step-by-step procedure in the form of flowchart has also been formulated and the developed design process with the experimental results has been validated.

A mathematical modeling of HT was reviewed and developed for assessing the successful working of the proposed system under the dynamic variation of the consumer load. The mechanical power output versus rotor speed characteristics of the HT for different water flow rates are also presented for driving a three-phase, 3.7 kW IGEC. From these characteristics, two operating regions are identified based on load voltage and frequency requirement of the consumer. For supplying a specific load at the generator terminals, the operating regions of the proposed system are also clearly presented. The overall system comprising of HT, IGEC, consumer and FLs along with the closed loop control scheme has been implemented using MATLAB/Simulink software to assess its steady state as well as dynamic performance. The stator line voltage has been taken as the control parameter and its value is maintained within the upper and lower bands by automatically turning on and off the FLs for any alterations in the consumer load. The functionality of the system for various operating conditions are noticed through simulation. Predetermined and simulated results for typical cases

are substantiated through the results obtained with experimental setup in the laboratory. The outcomes of the simulation, experiments, and predetermination all showed a high degree of agreement further confirms the successful functioning and usefulness of the proposed method of operating HT driven IGEC to be utilized for powering people living in remote sites.

Disclosure and Conflicts of Interest

The authors declare that they have no known competing financial interests or personal relationships that could have appeared to influence the work reported in this paper.

Acknowledgements

The authors warmly acknowledge the authorities of the National Institute of Technology, Tiruchirappalli, India, for all the facilities made available for doing the simulation and experimental work necessary for the development of this research work. The authors would also like to extend their sincere thanks to Dr. M. Subbiah for his valuable assistance in the preparation of presented research work.

References

[1] Renewables 2021: Analysis and forecast to 2026, IEA (2021), OECD Publishing, Paris, https://doi.org/10.1787/6dcd2e15-en.

[2] C.P. Jawahar, Prawin Angel Michael, 'A review on turbines for micro hydro power plant', Renewable and Sustainable Energy Reviews, vol. 72, pp. 882–887, May 2017.

[3] A.H. Elbatran, O.B. Yaakob, Yasser M. Ahmed, H.M. Shabara, 'Operation, performance and economic analysis of low head micro-hydropower turbines for rural and remote areas: A review', Renewable and Sustainable Energy Reviews, vol. 43, pp. 40–50, May 2015.

[4] Hossein Iman-Eini, David Frey, Seddik Bacha, Cedric Boudinet, Jean-Luc Schanen, ' Evaluation of loss effect on optimum operation of variable speed micro-hydropower energy conversion systems', Renew. Energy, vol. 131, pp. 1022–1034, Feb.2019.

[5] Baoling Guo, Seddik Bacha, Mazen Alamir, Amgad Mohamed, Boudinet C, 'LADRC applied to variable speed micro-hydro plants:

experimental validation', Control Engineering Practice, vol. 85, pp. 290–298, Apr. 2019.

[6] L. Belhadji, S. Bacha, I. Munteanu, A. Rumeau and D. Roye, 'Adaptive MPPT Applied to Variable-Speed Microhydropower Plant', IEEE Transactions on Energy Conversion, vol. 28, no. 1, pp. 34–43, Mar. 2013.

[7] J. L. Marquez, M. G. Molina, and J. M. Pacas, 'Dynamic modeling, simulation and control design of an advanced micro-hydro power plant for distributed generation applications', International Journal on Hydrogen Energy, vol. 35, Iss. 11, pp. 5772–5777, Jun. 2010.

[8] Shalvi Tyagi, Bhim Singh and Souvik Das, 'ELD-OSG Control of a Battery-Based Electronic Load Controller for a Small Hydro Energy Conversion System', IEEE Transactions on Industry Applications, vol. 58, no. 3, pp. 3142–3152, Jun. 2022.

[9] R. Raja Singh, B. Anil Kumar, D. Shruthi, Ramraj Panda and C. Thanga Raj, 'Review and experimental illustrations of electronic load controller used in standalone Micro-Hydro generating plants', Engineering Science and Technology, an International Journal, vol. 21, Iss. 5, pp. 886–900, Oct.2018.

[10] I. Sami, N. Ullah, S. M. Muyeen, K. Techato, M. S. Chowdhury and J.-S. Ro, 'Control Methods for Standalone and Grid Connected Micro-Hydro Power Plants With Synthetic Inertia Frequency Support: A Comprehensive Review', IEEE Access, vol. 8, pp. 176313–176329, Sep. 2020.

[11] V. B Murali Krishna, V. Sandeep, S.S. Murthy, Kishore Yadlapati, 'Experimental investigation on performance comparison of self excited induction generator and permanent magnet synchronous generator for small scale renewable energy applications', Renew. Energy, vol. 195, pp. 431–441, Jun. 2022.

[12] Krishna, V.B., and Sandeep, V., 'Experimental Investigations on Loading Capacity and Reactive Power Compensation of Star Configured Three Phase Self Excited Induction Generator for Distribution Power Generation', Distributed Generation & Alternative Energy Journal, Vol. 37(3), pp. 725–748, 2022.

[13] Praveen Kumar, Ujjwal Kumar Kalla, Nikhil Bhati, and Kusum Lata Agarwal, 'Performance Investigation of Synchronized Three-Phase AC Chopper-Based Controller for Small Hydrogeneration Systems', IEEE Transactions on industry applications, vol. 58, no. 2, pp. 2217–2228, Apr. 2022.

[14] Juan M. Ramirez, E.M. Torres, 'An electronic load controller for the self-excited induction generator', IEEE Transactions on Energy Conversion vol. 22, no. 2, pp. 546–548, Jun. 2007.
[15] Babak Nia Roodsar and Edwin Peter Nowicki, 'Analysis and Experimental Investigation of the Improved Distributed Electronic Load Controller', IEEE Transactions on Energy Conversion, vol. 33, no. 3, pp. 905–914, Sep. 2018.
[16] Bhim Singh, S. S. Murthy, and Sushma Gupta, 'Analysis and design of electronic load controller for self-excited induction Generators', IEEE Transactions on Energy Conversion, vol. 21, no. 1, pp. 285–293, Mar. 2006.
[17] Valluri Chandra Sekhar, Krishna Kant, and Bhim Singh, 'DSTATCOM supported induction generator for improving power quality'. IET Renew. Power Gener., vol. 10, Iss. 4, pp. 495–503, 2016.
[18] Scherer L.G., Tambara R.V., de Camargo R.F, 'Voltage and frequency regulation of standalone self-excited induction generator for micro-hydropower generation using discrete-time adaptive control', IET Renew. Power Gener., vol. 10, Iss. 4, pp. 531–540, 2016.
[19] Rajasekhara Reddy Chilipi, Bhim Singh and S. S. Murthy, 'Performance of a Self-Excited Induction Generator With DSTATCOM-DTC Drive-Based Voltage and Frequency Controller', IEEE Transactions on Energy Conversion, vol. 29, no. 3, pp. 545–557, Sep. 2014.
[20] Scherer L.G., C.B. Tischer, de Camargo R.F, 'Power rating reduction of distribution static synchronous compensator for voltage and frequency regulation of stand-alone self-excited induction generator', Electric Power Systems Research, vol. 149, pp. 198–209, Aug. 2017.
[21] J. A. Barrado, R. Grino and H. Valderrama-Blavi, 'Power-Quality Improvement of a Stand-Alone Induction Generator Using a STATCOM With Battery Energy Storage System', IEEE Transactions on Power delivery, vol. 25, no. 4, pp. 2734–2741, Oct. 2010.
[22] Sachin Tiwari, Seema Kewat, Bhim Singh, Chandrakala Devi Sanjenbam, 'Battery-supported unified power quality controller for small hydro-based isolated power generation', IET Renew. Power Gener., vol. 15, pp. 2160–2167, Jan. 2021.
[23] V. Nayanar, N. Kumaresan, and N. A. Gounden, 'A Single-Sensor-Based MPPT Controller for Wind-driven Induction Generators Supplying DC Microgrid', IEEE Transactions on Power Electronics, vol. 31, no. 2, pp. 1161–1172, Feb. 2016.

[24] K. Arthishri, K. Anusha, N. Kumaresan, and S. S. Kumar, 'Simplified methods for the analysis of self-excited induction generators', IET Electric Power Appl., vol. 11, no. 9, pp. 1636–1644, Nov. 2017.
[25] K. Arthishri, N. Kumaresan, and N. A. Gounden, 'Analysis and application of three-phase SEIG with power converters for supplying single-phase grid from wind energy', IEEE Systems Journal, vol. 13, no. 2, pp. 1813–1822, Jun. 2019.
[26] S. Kumar, V. Krishnasamy and R. Kaur, 'Unified Controller for Bimodal Operation of Cuk Converter Assisted SEIG-Based DC Nanogrid', IEEE Systems Journal, vol. 15, no. 2, pp. 1674–1683, Jun. 2021.
[27] Chatterjee, H.S., and Mahato, S.N., 'A New and Simple Mathematical Technique to Study the Steady-state Performance of Isolated Asynchronous Generator', Distributed Generation & Alternative Energy Journal, Vol.37_3, pp. 663–682, 2022.
[28] M. S. Akbarali, S. Subramaniam, and K. Natarajan, 'Application of CS-PWM rectifier for the operation and control of wind-driven generators', Energy Sources, Part A: Recovery, Utilization, and Environmental Effects, pp. 1–17, 2020.
[29] S. S. Kumar, N. Kumaresan, M. Subbiah, and M. Rageeru, 'Modelling, analysis and control of stand-alone self-excited induction generator-pulse width modulation rectifier systems feeding constant DC voltage applications', IET Gener., Transmiss. Distrib., vol. 8, Iss. 6, pp. 1140–1155, Jun. 2014.
[30] Rashid, M., Alotaibi, M.A., Chowdhury, A.H., Rahman, M., Alam, M.S., Hossain, M.A., and Abido, M.A, 'Home Energy Management for Community Microgrids Using Optimal Power Sharing Algorithm', Energies 2021, 14, 1060, pp. 1–21.
[31] Arun S. and Manickavasagam Parvathy Selvan, 'Dynamic demand response in smart buildings using an intelligent residential load management system', IET Gener. Transmiss. Distrib., vol. 11, Iss. 17, pp. 4348–4357, 2017.
[32] Aijaz, M., Hussain, I., and Lone, S. A. 'Priority Based Critical Load Selection Algorithm for Grid Integrated PV Powered EV Charging System with Optimal DC Link Control'. Distributed Generation & Alternative Energy Journal, 2022, 38(01), 293–318. https://doi.org/10.13052/dgaej2156-3306.38113.

Biographies

Hanumanthu Kesari received his B.Tech. degree in Electrical and Electronics Engineering from Rajeev Gandhi Memorial College of Engineering and Technology, Nandyala, India and M.Tech. degree in power electronics from B.M.S. College of Engineering, Bangalore, India. He is currently pursuing his Ph.D degree from NIT, Tiruchirappalli. His research areas include electrical machines and drives, renewable energy systems.

Natarajan Kumaresan received his B.E. degree from Bangalore University, Bangalore, India, in 1992, and the M.E. degree in power systems from the National Institute of Technology (then Regional Engineering College), Tiruchirappalli, India, in 1994, and the Ph.D. degree from Bharathidasan University, Tiruchirappalli, India, in 2005. Since 1999, he has been with the Department of Electrical and Electronics Engineering, National Institute of Technology, Tiruchirappalli, where he is currently a professor. His research

interests include design and development of electrical machines and power electronic controllers for renewable energy electric conversion systems. Dr. Kumaresan received the Career Award for Young Teachers in December 2006, instituted by the All India Council for Technical Education, Government of India. He is a Senior Member of IEEE, a Member of the IET, UK, Fellow of the Institution of Engineers, India and Life Member of the ISTE.